

An Approach to Estimate the Barrier Height for Magnetization Reversal in {Dy₂} SMMs Using Ab initio Calculations

Sourav Dey and Gopalan Rajaraman*

Computational Details:

The relationship between structure and magnetic properties is a critical aspect of molecular magnetism. Sometimes the ferromagnetic to antiferromagnetic transition with structure is not clear. In this regard, *ab initio* calculation plays a significant role to predict the magnetic coupling. First, the CASSCF/RASSI-SO/SINGLE_ANISO¹ calculation is being performed with CAS(9,7) active space on each one Dy(III) centres with replacing the neighbouring Dy(III) ion with a diamagnetic analogue such as Lu in MOLCAS programme package.²⁻⁵ The basis set for the calculation has been taken from the ANO-RCC library implemented in the MOLCAS programme package.² The calculation provides the single-ion anisotropy of the individual Dy(III) centre. Thereafter, the metal ions are coupled using POLY_ANISO to estimate the magnetic exchange.⁶ It interfaces with the single-ion anisotropy information of the metal ions from SINGLE_ANISO to fit the temperature-dependent magnetic susceptibility ($\chi_M T$ vs T) and field dependent magnetisation (M vs H). A good fit in the corresponding plot yields the correct magnetic exchange. The magnetic exchange is computed by the following two Hamiltonian, $\hat{H} = -J_{lines} \hat{S}_1 \hat{S}_2$ and $\hat{H} = -J_{Ising} \hat{S}_{z1} \hat{S}_{z2}$. The first one uses true spin ($S = 5/2$) of the Dy(III) ions to compute the magnetic exchange using lines model while the second one uses pseudospin ($S = 1/2$) of the Dy(III) ions to calculate the magnetic exchange between Dy(III) ions considering the Ising interaction.^{7, 8} Therefore the computed exchange from the two models is related to a factor of 25. In our manuscript, we have followed the first formalism (lines model) if not mentioned otherwise.

Classification of Dy dimer based on ligand backbone and bridging group:

Table S1: The $\{\text{Dy}_2\}$ SMM with U_{eff} and computed relaxation parameters (all values in cm^{-1}).

The QTM/TA-QTM of the $(x-1)^{\text{th}}$ KD has been provided if it relaxes via x^{th} KD.

Class	Complex (CSD ref Code)	Local Symmetry	U_{eff}	$U_{\text{cal}}(\text{Dy1})$	$U_{\text{cal}}(\text{Dy2})$	QTM/TA-QTM (Dy1)	QTM/TA-QTM (Dy2)	J	U_{caleff}	Ref
a	$[(\eta^5\text{-Cp})_2(\text{thf})\text{Dy}(\mu\text{-Cl})_2$ (1 , XAMBOE)	D_{3h}	34.0	97.6	97.6	0.0093	0.0093	- 0.076	19.8	9
a	$[(\eta^5\text{-Cp})_2\text{Dy}(\mu\text{-Cl})_2$ (2 , XAMCAR)	T_d	26.0	383.4	383.4	0.0148	0.0148	- 0.103	50.3	9
a	$[\{\text{Cp}'_2\text{Dy}(\mu\text{-SSiPh}_3)\}_2]$ (3 , TEFZOV)	T_d	133.0	241.1	241.1	0.0022	0.0022	- 0.176	216.6	10
a	$[(\text{PyCp}_2)_2\text{Dy}(\mu\text{-O}_2\text{SOCF}_3)_2$ (4 , FEBTAK)	D_{3h}	49.0	138.0	138.0	0.0056	0.0056	0.005	49.4	11
a	$[(\text{PyCp}_2)_2\text{Dy}(\mu\text{-Cl})_2$ (5 , FEBFAW)	D_{3h}	49.0	134.0	134.0	0.0051	0.0051	- 0.005	52.5	11
a	$[\text{Cp}'_2\text{Dy}(\mu\text{-Cl})_2]$ (6 , GUXQAU)	T_d	106.0	273.0	273.0	0.0044	0.0044	- 0.170	121.5	12
a	$[\text{Cp}'_2\text{Dy}(\mu\text{-I})_2]$ (7 , GUXQEY)	T_d	341.0	429.3	429.3	0.0080	0.0080	- 0.153	105.0	12
a	$[\text{Dy}_2\text{Cp}^*_4(\mu\text{-BPh}_4)]$ (8 , VUQHIB)	C_{3v}	330.0	462.0	462.0	0.0026	0.0026	0.001	355.4	13
a	$[\{\text{Dy}(\text{Cp}^*)_2(\mu\text{-Me}_3\text{AlNEt}_3)\}_2]$ (9 , HULRAK)	T_d	860.0	680.8	680.8	0.0016	0.0016	0.420	857.3	14
b	$[\text{Dy}^{\text{III}}_2(\text{valdien})_2(\text{NO}_3)_2]$ (10 , IYILOS)	D_{2d}	52.8	201.7	201.7	0.0049	0.0049	- 0.210	79.2	15
b	$[\text{Dy}_2(\text{valdien})_2(\text{CH}_3\text{COO})_2]$ (11 , DOCQIX)	D_{2d}	23.6	138.0	138.0	0.0069	0.0069	- 0.152	37.7	16
b	$[\text{Dy}_2(\text{valdien})_2(\text{ClCH}_2\text{COO}^-)_2]$ (12 , DOCQOD)	D_{2d}	34.7	152.0	152.0	0.0080	0.0080	- 0.248	34.3	16
b	$[\text{Dy}_2(\text{valdien})_2(\text{Cl}_2\text{CHCOO}^-)_2]$ (13 , DOCQUJ)	D_{2d}	41.7	154.0	154.0	0.0167	0.0167	- 0.248	14.7	16
b	$[\text{Dy}_2(\text{valdien})_2(\text{CH}_3\text{COCHCOCH}_3^-)_2]$ (14 , DOCRAQ)	D_{2d}	11.1	22.0	22.0	0.0024	0.0024	- 0.094	16.9	16
b	$[\text{Dy}_2(\text{opvh})_2\text{Cl}_2(\text{MeOH})_3]$ (15 , AXEQAW)	D_{5h} (Dy1) D_{2d} (Dy2)	120.5*	321.1	190.5	0.0349	0.0014	0.235	148.8	4
b	$[\text{Dy}_2(\text{opch})_2(\text{OAc})_2(\text{H}_2\text{O})_2]$ (16 , TEYDAF)	D_{2d}	95.2	191.7	191.7	0.0033	0.0033	0.185	118.9	17
b	$[\text{Dy}_2(\text{L})_2(\text{NO}_3)_4(\text{CH}_3\text{OH})_2]$ (17 , TIJAA)	D_{3h}	52.8	118.1	118.1	0.0034	0.0034	- 0.250	65.7	18
b	$[\text{Dy}(\text{opch})\text{Cl}(\text{MeOH})_2]$ (18 , TIJAA)	D_{5h}	54.0	196.1	196.1	0.0067	0.0067	0.088	59.8	19
b	$[\text{Dy}_2(\text{L}_1)_2(\text{L}')_2(\text{CH}_3\text{OH})_2]$ (19 , DALXOG)	D_{4d}	47.9	159.1	159.1	0.0072	0.0072	0.090	45.6	20
b	$[\text{Dy}_2(\text{L}_2)_2(\text{L}')_2(\text{CH}_3\text{OH})_2]$ (20 , DALYEX)	D_{4d}	35.4	159.4	159.4	0.0122	0.0122	0.330	31.1	20
b	$[\text{Dy}_2(\text{NO}_3)_4(\text{sacbH})_2(\text{H}_2\text{O})_2(\text{MeCN})_2]$ (21 , YAWHAI)	D_{3h}	75.9	149.3	149.3	0.0035	0.0035	- 0.003	85.3	21
b	$[\text{Dy}_2\text{L}_2(\text{OAc})_4(\text{MeOH})_2]$ (22 , LULDII)	D_{2d}	90.0	181.9	181.9	0.0037	0.0037	- 0.126	96.4	22
c	$[(\text{NN}^{\text{TBS}})\text{Dy}]_2(\mu\text{-biphenyl})[\text{K-}(\text{solvent})_2]$ (23 , POXMAS)	D_{3h}	23.5	90.4	90.4	0.0212	0.0212	- 0.060	7.6	23
c	$[\text{KDy}_2(\text{C}_7\text{H}_7)(\text{N}(\text{SiMe}_3)_2)_2]$ (24 , SENJON)	D_{3h} (Dy1) C_{2v} (Dy2)	40.2*	115.9	69.1	0.0047	0.0019	0.781	72.7	24
d	$[\text{Dy}(\text{Me}_5\text{trenCH}_2)(\mu\text{-H}_3)\text{Dy}(\text{Me}_6\text{tren})]$ (25 , NERZUH)	C_{3v} (Dy1) D_{2d} (Dy2)	40.0	94.0	231.0	0.0331	0.0081	- 0.098	29.9	25
d	$[\text{Dy}(\text{Cy}_2\text{N})_2(\mu\text{-Cl})(\text{THF})_2]$ (26 , GOMTIO)	D_{3h}	433.0	466.5	466.5	0.0040	0.0040	-	233.0	26

									0.018		
e	$[(\mu\text{-mbpymNO})\text{-}\{(\text{tmh})_3\text{Dy}\}_2]$ (27, VEZTIG)	$\text{D}_{2\text{d}}(\text{Dy1})$ $\text{D}_{4\text{d}}(\text{Dy2})$	35.6*	109.7	157.2	0.0200	0.0030	- 0.070	56.8	27	
e	$[(\mu\text{-bipym})\{((+)\text{-tfacam})_3\text{Dy}\}_2]$ (28, YUDBUX)*	$\text{D}_{4\text{d}}$	38.2	141.9	129.9	0.0034	0.0100	0.004	54.8	28	
e	$[(\mu\text{-bipym})\{(\text{Dbzm})_3\text{Dy}\}_2]\cdot 2\text{CH}_3\text{Cl}$ (29, UMITOB)	$\text{D}_{2\text{d}}(\text{Dy1})$ $\text{D}_{4\text{d}}(\text{Dy2})$	93.1*	183.8	157.4	0.2800	0.0017	- 0.040	92.6	29	
e	$[(\mu\text{-bipym})\{(\text{Dbzm})_3\text{Dy}\}_2]\cdot \text{MeCN}$ (30, UMITUH)	$\text{D}_{2\text{d}}$	185.4	170.8	170.8	0.0035	0.0035	0.006	97.6	29	
e	$[\text{Dy}_2(\text{bpm})(\text{tfaa})_6]$ (31, XOPLIA)	$\text{D}_{4\text{d}}$	22.9	101.5	101.5	0.0057	0.0057	- 0.046	34.9	30	

* The U_{eff} value has been provided as an average from the two-relaxation process called FR and SR.

Abbreviations of all the complexes have been given in the Figure caption (below, Figure S1-S32)

(a) Dimers with cyclopentadienyl ligand:

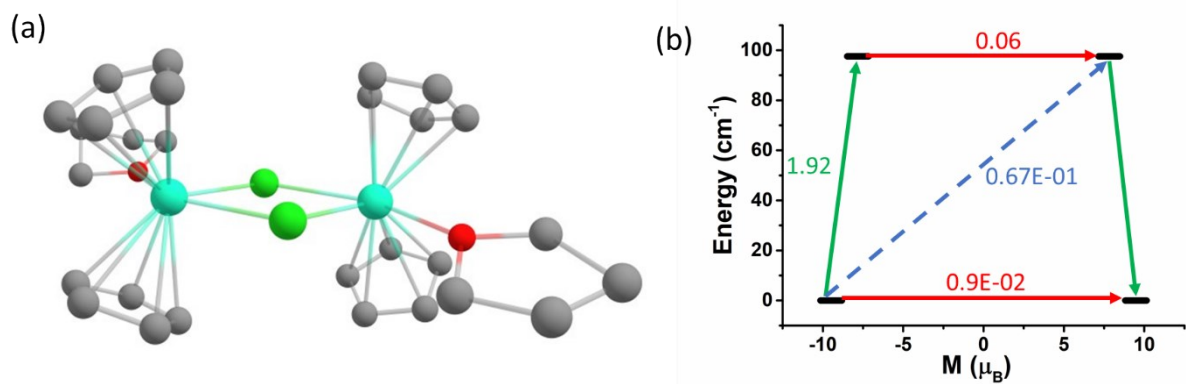


Figure S1: (a) Molecular structure of $[(\eta^5\text{-Cp})_2(\text{thf})\text{Dy}(\mu\text{-Cl})]_2$ (**1**).⁹ Colour code: Dy-aqua, Cl-green, O-red, C-grey. Hydrogens are omitted for clarity. (b) Mechanism of relaxation of Dy1 center of **1** (Dy2 center is equivalent to Dy1 center). The Dy1 center relaxes via 1st excited KD due to the large angle (17.1°) of the anisotropy axis with respect to ground state despite of small TA-QTM at this level. The red arrows indicate the QTM or TA-QTM via ground or excited KD, respectively. The sky dotted arrows shows the mechanism of Orbach process. The olive arrows indicate the pathway of magnetic relaxation.

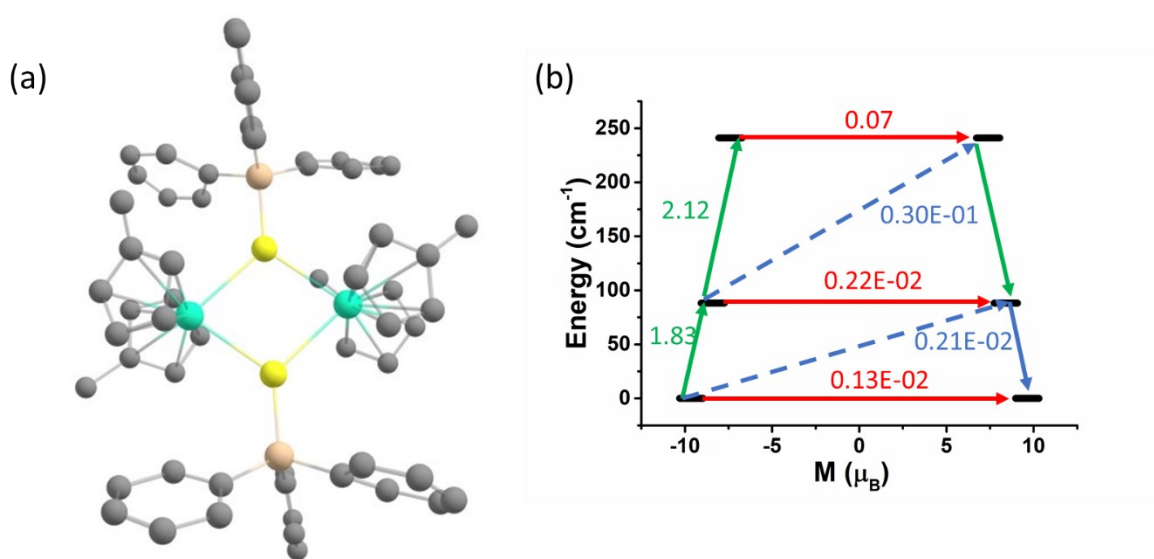
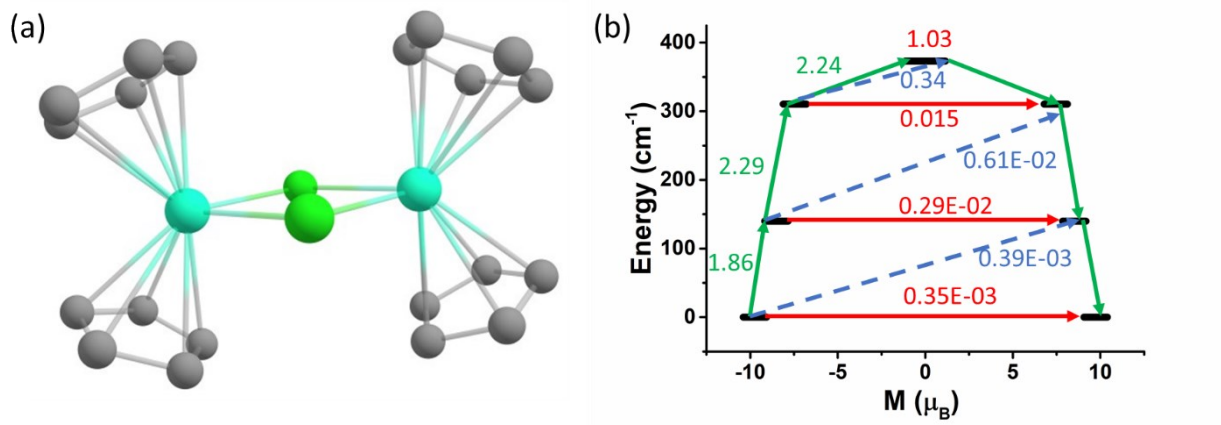


Figure S3: (a) Molecular structure of $[\{\text{Cp}'_2\text{Dy}(\mu\text{-SSiPh}_3)\}_2]$ (**3**, $\text{Cp}'=\eta^5\text{-C}_5\text{H}_4\text{Me}$).¹⁰ Colour code: Dy-aqua, S-yellow, Si-maple, C-grey. Hydrogens are omitted for clarity. (b) Mechanism of relaxation of Dy1 center of **3** (Dy2 center is equivalent to Dy1 center). The Dy1 center relaxes via 2nd excited KD due to the large angle (16.7°) of the anisotropy axis with respect to ground state despite of small TA-QTM at this level. The red arrows indicate the QTM or TA-QTM via ground or excited KD, respectively. The sky dotted arrows shows the mechanism of Orbach process. The olive arrows indicate the pathway of magnetic relaxation.

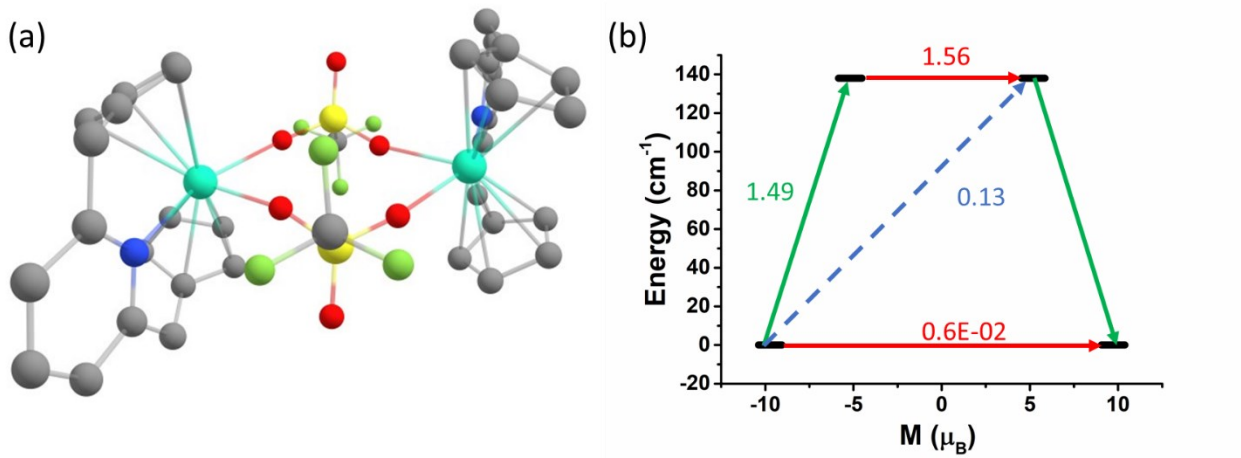


Figure S4: (a) Molecular structure of $[(\text{PyCp}_2)\text{Dy}(\mu\text{-O}_2\text{SOCF}_3)]_2$ (**4**).¹¹ Colour code: Dy-aqua, S-yellow, Si-maple, F-lime green, N-blue, O-red, C-grey. Hydrogens are omitted for clarity. (b) Mechanism of relaxation of Dy1 center of **4** (Dy2 center is equivalent to Dy1 center). The red arrows indicate the QTM or TA-QTM via ground or excited KD, respectively. The sky dotted arrows shows the mechanism of Orbach process. The olive arrows indicate the pathway of magnetic relaxation.

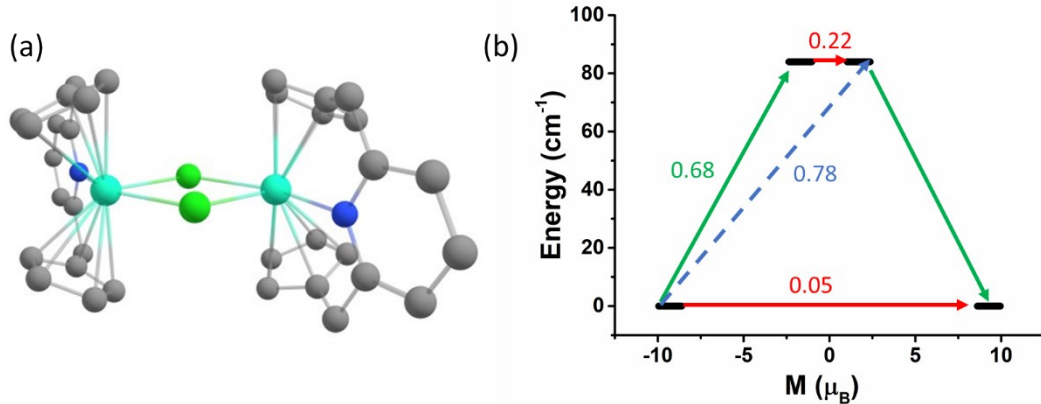


Figure S5: (a) Molecular structure of $[(\text{PyCp}_2)\text{Dy}(\mu\text{-Cl})]_2$ (**5**).¹¹ Colour code: Dy-aqua, Cl-green, N-blue, C-grey. Hydrogens are omitted for clarity. (b) Mechanism of relaxation of Dy1 center of **5** (Dy2 center is equivalent to Dy1 center). The red arrows indicate the QTM or TA-QTM via ground or excited KD, respectively. The sky

dotted arrows shows the mechanism of Orbach process. The olive arrows indicate the pathway of magnetic relaxation.

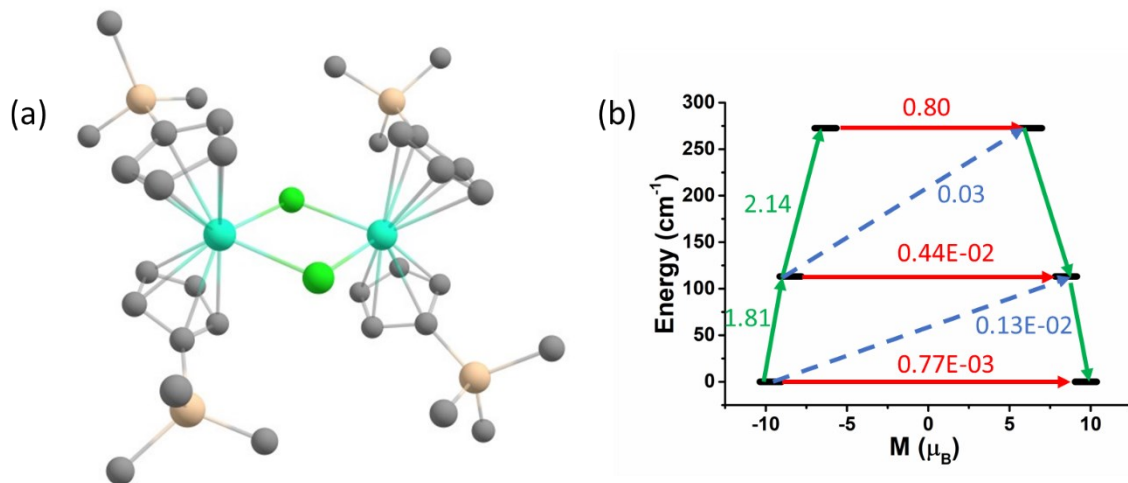


Figure S6: (a) Molecular structure of $[\text{Cp}'_2\text{Dy}(\mu\text{-Cl})]_2$ (6, Cp' = cyclopentadienyltrimethylsilane anion).¹² Colour code: Dy-aqua, Cl-green, Si-maple, N-blue, C-grey. Hydrogens are omitted for clarity. (b) Mechanism of relaxation of Dy1 center of 6 (Dy2 center is equivalent to Dy1 center). The red arrows indicate the QTM or TA-QTM via ground or excited KD, respectively. The sky dotted arrows shows the mechanism of Orbach process. The olive arrows indicate the pathway of magnetic relaxation.

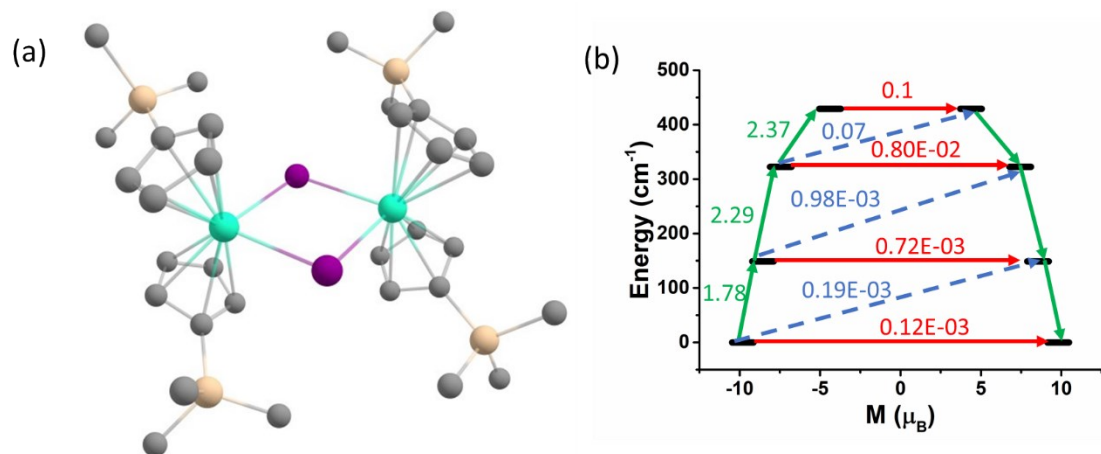


Figure S7: (a) Molecular structure of $[\text{Cp}'_2\text{Dy}(\mu\text{-I})_2]$ (7, Cp' = cyclopentadienyltrimethylsilane anion).¹² Colour code: Dy-aqua, I-violet, Si-maple, N-blue, C-grey. Hydrogens are omitted for clarity. (b) Mechanism of relaxation of Dy1 center of 7 (Dy2 center is equivalent to Dy1 center). The red arrows indicate the QTM or TA-QTM via ground or excited KD, respectively. The sky dotted arrows shows the mechanism of Orbach process. The olive arrows indicate the pathway of magnetic relaxation.

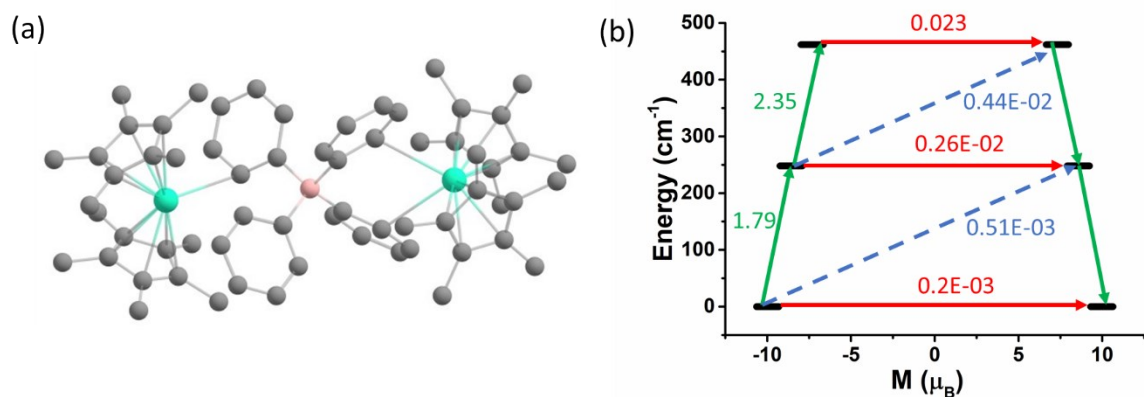


Figure S8: (a) Molecular structure of $[\text{Dy}_2\text{Cp}^*_4(\mu\text{-BPh}_4)]$ (8, Cp^* = 1,2,3,4,5-Pentamethylcyclopentadiene).¹³ Colour code: Dy-aqua, B-light pink, C-grey. Hydrogens are omitted for clarity. (b) Mechanism of relaxation of Dy1 center of 8 (Dy2 center is equivalent to Dy1 center). The Dy1 center relaxes via 2nd excited KD due to the large angle (5.8°) of the anisotropy axis with respect to ground state despite of small TA-QTM at this level. The red arrows indicate the QTM or TA-QTM via ground or excited KD, respectively. The sky dotted arrows shows the mechanism of Orbach process. The olive arrows indicate the pathway of magnetic relaxation.

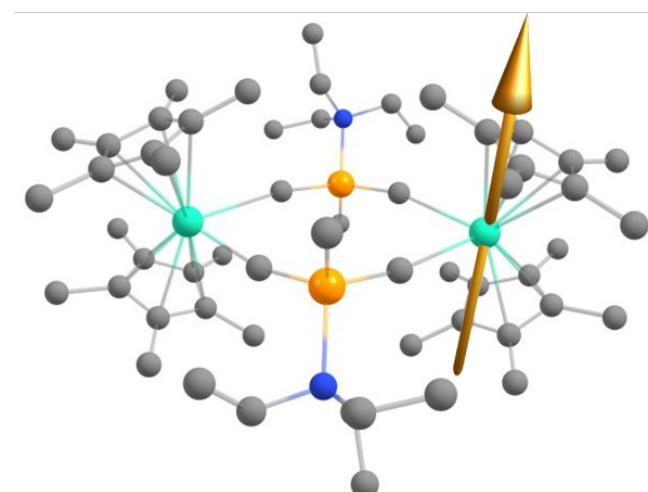


Figure S9: The ground state anisotropy axis of Dy1 center of **9**.¹⁴ Colour code: Dy-aqua, Al-amber, N-blue, C-grey. Hydrogens are omitted for clarity. Mechanism of magnetic relaxation of Dy1 center is given in the main manuscript.

Table S2: The g tensors of eight KDs along with energy (cm⁻¹) of Dy1 centre of **9** (Dy2 centre is symmetric to Dy1).

Energy (cm ⁻¹)	g _x	g _y	g _z	Angle of g _{zz} between ground and higher excited KDs (°)
0.0	0.000	0.000	19.848	
296.4	0.002	0.002	17.089	0.8
526.9	0.005	0.008	14.544	0.8
681.6	0.138	0.148	11.862	6.0
791.2	1.674	2.446	8.617	7.2
841.6	10.115	7.132	2.877	3.0
906.8	0.506	1.554	14.922	89.3
1106.4	0.029	0.045	19.480	89.3

(b) Dimer with Schiff base linkage:

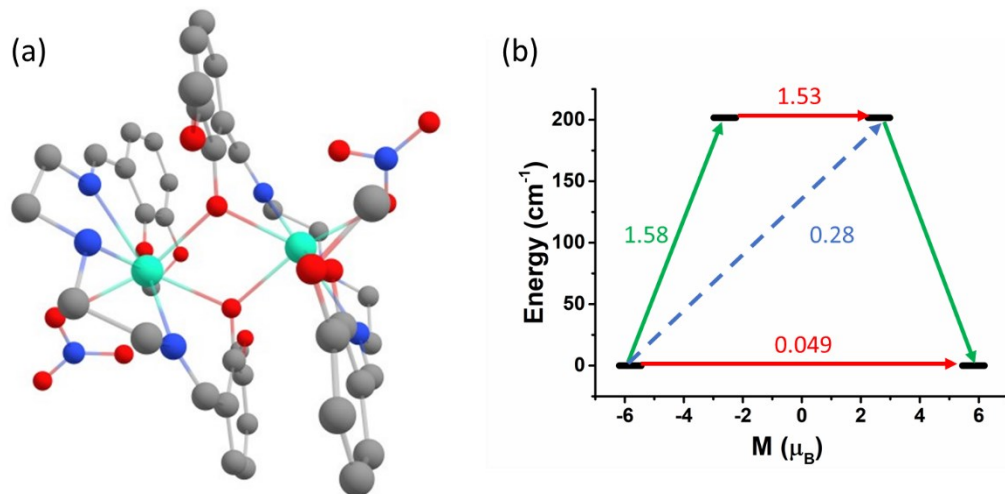


Figure S10: (a) Molecular structure of $[\text{Dy}^{\text{III}}_2(\text{valdien})_2(\text{NO}_3)_2]$ (**10**, $\text{H}_2\text{valdien} = \text{N}1,\text{N}3\text{-bis}(3\text{-methoxysalicylidene})\text{diethylenetriamine}$).¹⁵ Colour code: Dy-aqua, O-red, N-blue, C-grey. Hydrogens are omitted for clarity. (b) Mechanism of relaxation of Dy1 center of **10** (Dy2 center is equivalent to Dy1 center). The red arrows indicate the QTM or TA-QTM via ground or excited KD, respectively. The sky dotted arrows shows the mechanism of Orbach process. The olive arrows indicate the pathway of magnetic relaxation.

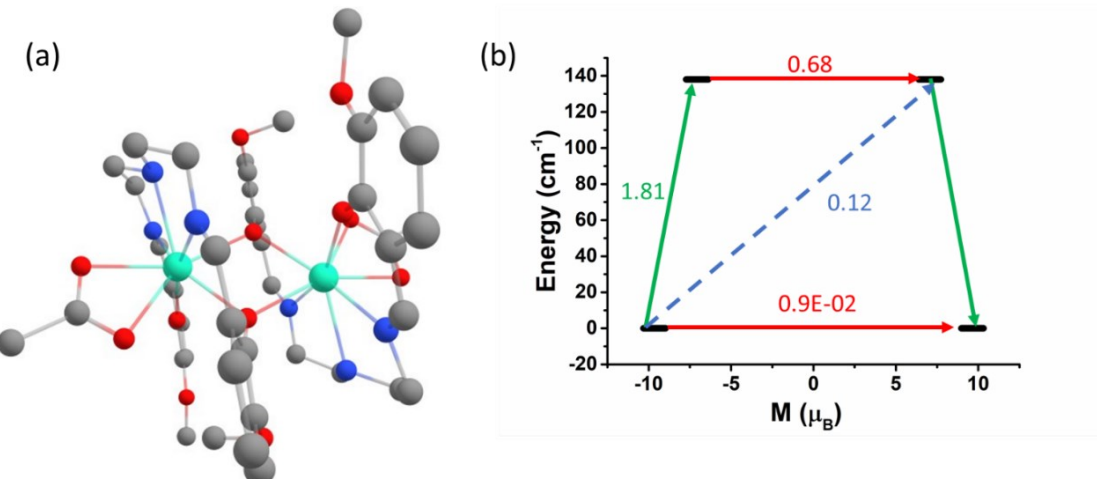


Figure S11: (a) Molecular structure of $[\text{Dy}_2(\text{valdien})_2(\text{CH}_3\text{COO})_2]$ (**11**).¹⁶ Colour code: Dy-aqua, O-red, N-blue, C-grey. Hydrogens are omitted for clarity. (b) Mechanism of relaxation of Dy1 center of **11** (Dy2 center is equivalent to Dy1 center). The red arrows indicate the QTM or TA-QTM via ground or excited KD, respectively. The sky dotted arrows shows the mechanism of Orbach process. The olive arrows indicate the pathway of magnetic relaxation.

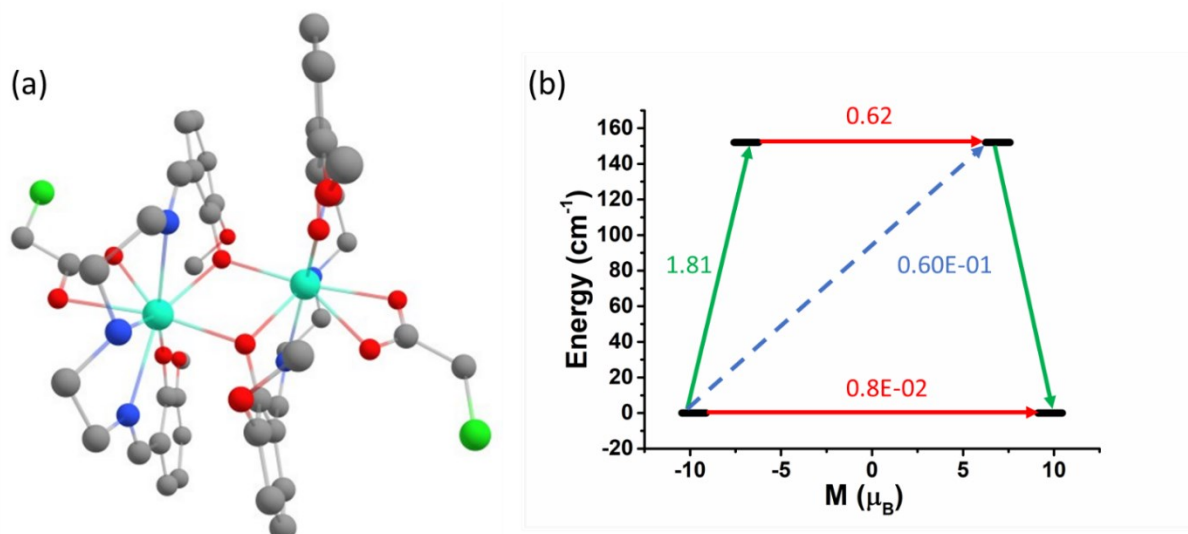


Figure S12: (a) Molecular structure of $[\text{Dy}_2(\text{valdien})_2(\text{ClCH}_2\text{COO}^-)_2]$ (**12**).¹⁶ Colour code: Dy-aqua, Cl-green, O-red, N-blue, C-grey. Hydrogens are omitted for clarity. (b) Mechanism of relaxation of Dy1 center of **12** (Dy2 center is equivalent to Dy1 center). The red arrows indicate the QTM or TA-QTM via ground or excited KD, respectively. The sky dotted arrows shows the mechanism of Orbach process. The olive arrows indicate the pathway of magnetic relaxation. The large blue arrow represents mechanism overall of magnetic relaxation.

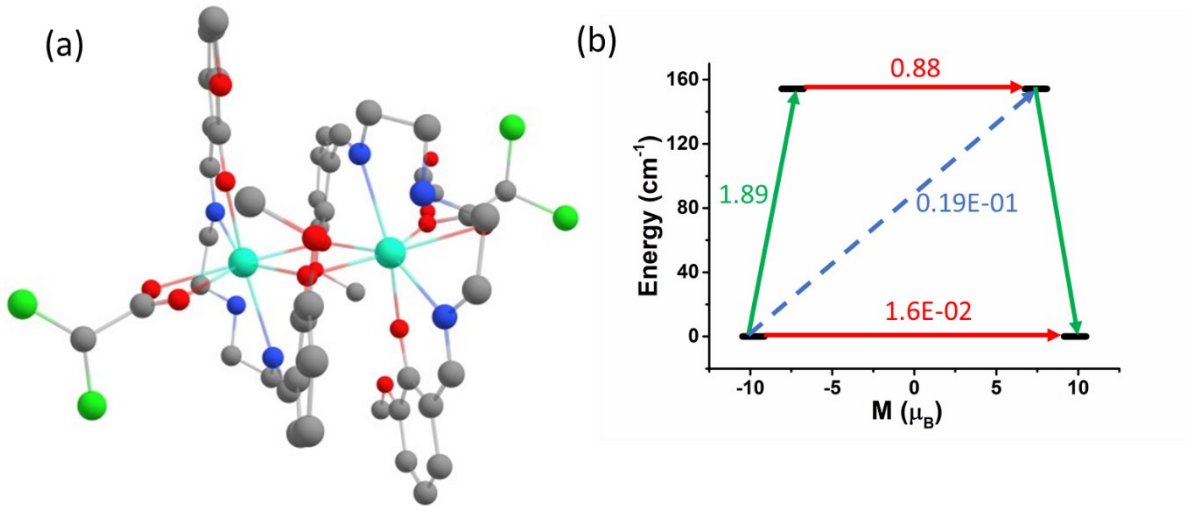


Figure S13: (a) Molecular structure of $[\text{Dy}_2(\text{valdien})_2(\text{Cl}_2\text{CHCOO}^-)_2]$ (**13**).¹⁶ Colour code: Dy-aqua, Cl-green, O-red, N-blue, C-grey. Hydrogens are omitted for clarity. Mechanism of relaxation of Dy1 center of **13** (Dy2 center is equivalent to Dy1 center). The red arrows indicate the QTM or TA-QTM via ground or excited KD, respectively. The sky dotted arrows shows the mechanism of Orbach process. The olive arrows indicate the pathway of magnetic relaxation.

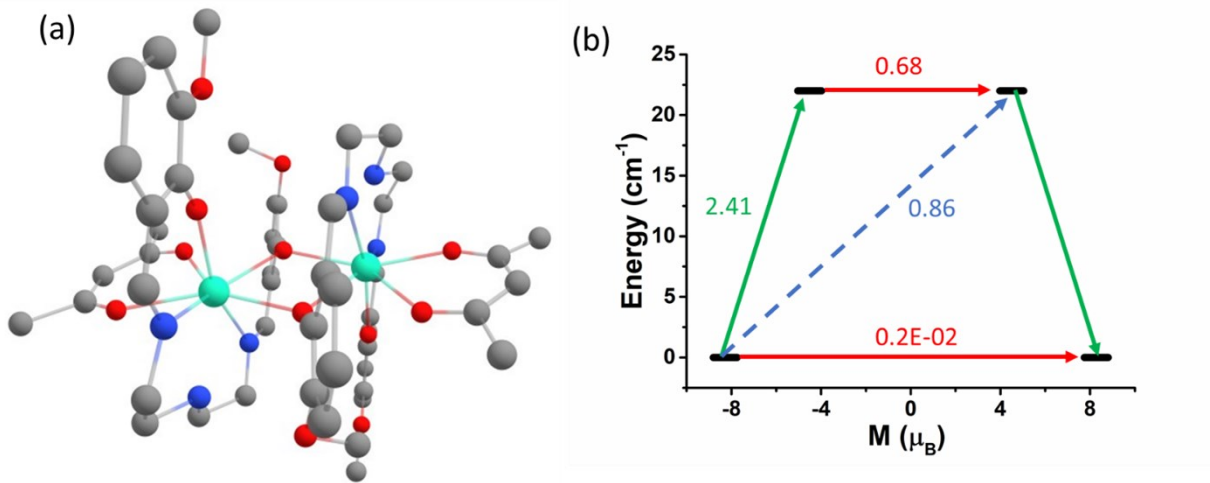


Figure S14: (a) Molecular structure of $[\text{Dy}_2(\text{valdien})_2(\text{CH}_3\text{COCHCOCH}_3^-)_2]$ (**14**).¹⁶ Colour code: Dy-aqua, O-red, N-blue, C-grey. Hydrogens are omitted for clarity. (b) Mechanism of relaxation of Dy1 center of **14** (Dy2 center is equivalent to Dy1 center). The red arrows indicate the QTM or TA-QTM via ground or excited KD, respectively. The sky dotted arrows shows the mechanism of Orbach process. The olive arrows indicate the pathway of magnetic relaxation.

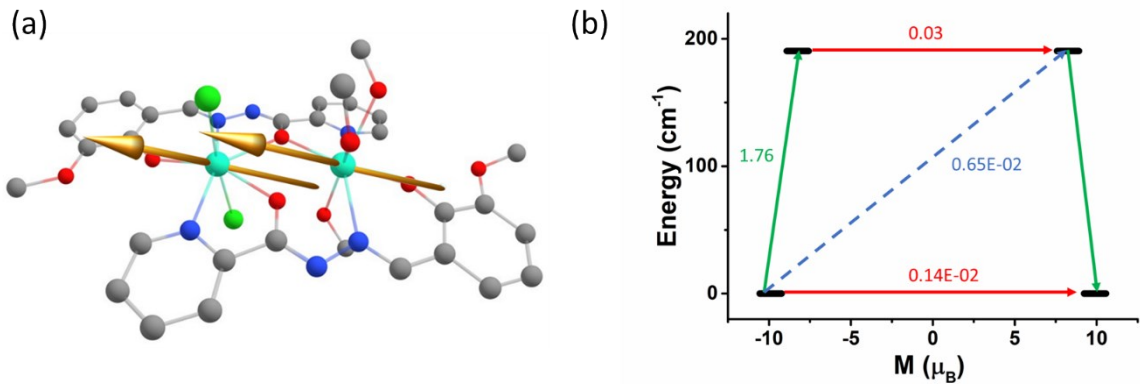


Figure S15: (a) The ground state anisotropy axis of the Dy centers in **15**.⁴ Colour code: Dy-aqua, F-lime green, O-red, N-blue, C-grey. Hydrogens are omitted for clarity. (b) Mechanism of relaxation of Dy2 center of **15** (the relaxation mechanism of Dy1 center is given in the main manuscript). The red arrows indicate the QTM or TA-QTM via ground or excited KDs, respectively. The olive arrows indicate the pathway of magnetic relaxation.

Table S3: The g tensors of four KDs along with energy (cm^{-1}) of Dy1 center of **15**.

Energy (cm^{-1})	g_x	g_y	g_z	Angle of g_{zz} between ground and higher excited KDs ($^\circ$)
0.0	0.001	0.001	19.779	
231.4	0.065	0.141	16.544	4.5
321.1	0.058	0.228	18.156	64.9
401.3	1.482	2.152	11.409	14.5
480.4	8.454	6.832	4.743	31.2
551.2	0.700	1.381	14.719	100.0
572.1	0.453	0.631	18.056	88.7
693.9	0.066	0.132	19.402	65.3

Table S4: The g tensors of four KDs along with energy (cm^{-1}) of Dy2 centre of **15**.

Energy (cm^{-1})	g_x	g_y	g_z	Angle of g_{zz} between ground and higher excited KDs ($^\circ$)
0.0	0.003	0.006	19.797	
190.5	0.076	0.087	17.232	16.8
390.3	0.772	1.587	13.214	7.3
464.3	10.776	8.454	2.587	8.3
507.1	0.666	5.900	12.655	90.1
569.9	8.805	6.076	2.484	61.5
635.5	1.789	2.435	16.814	81.2
694.1	0.378	0.682	18.977	92.3

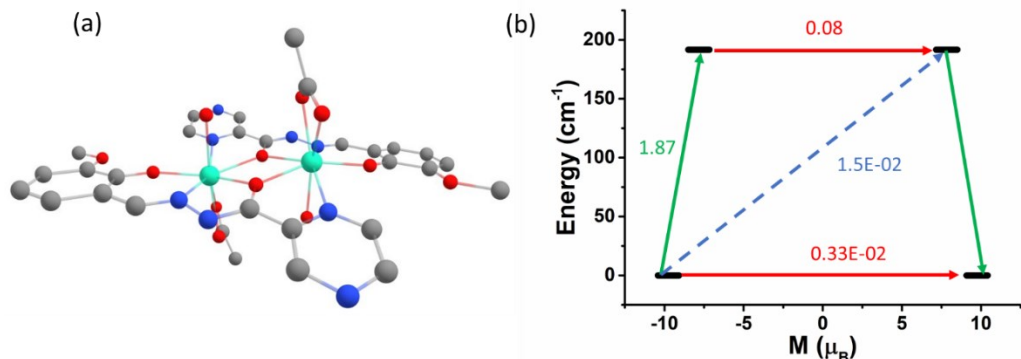


Figure S16: (a) Molecular structure of $[\text{Dy}_2(\text{opch})_2(\text{OAc})_2(\text{H}_2\text{O})_2]$ (16, $\text{opch} = (E)$ -N'-(2-hyborxy-3-methoxybenzylidene)pyrazine-2-carbohydrazide).¹⁷ Colour code: Dy-aqua, O-red, N-blue, C-grey. Hydrogens are omitted for clarity. (b) Mechanism of relaxation of Dy1 center of **16** (Dy2 center is equivalent to Dy1 center). The Dy1 center relaxes via 1st excited KD due to the large angle (16.5°) of the anisotropy axis with respect to ground state despite of small TA-QTM at this level. The red arrows indicate the QTM or TA-QTM via ground or excited KD, respectively. The sky dotted arrows shows the mechanism of Orbach process. The olive arrows indicate the pathway of magnetic relaxation.

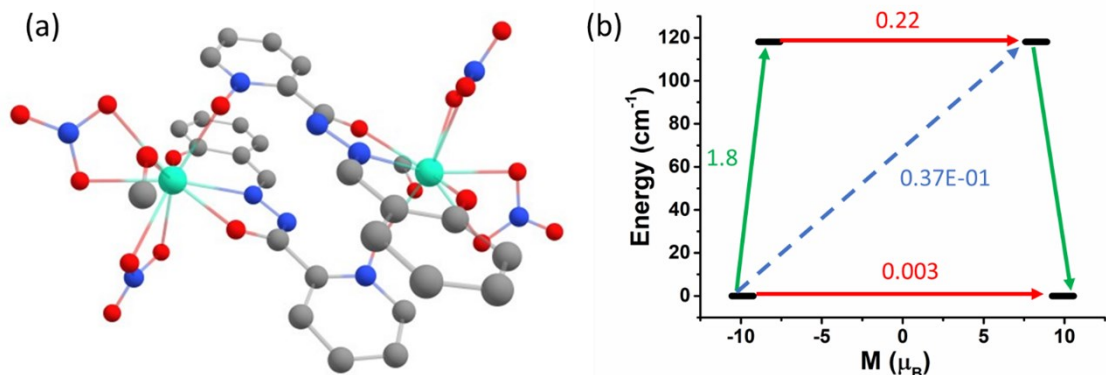


Figure S17: (a) Molecular structure of $[\text{Dy}_2(\text{L})_2(\text{NO}_3)_4(\text{CH}_3\text{OH})_2]$ (17, $\text{HL} = \text{N}'$ -(2-hydroxybenzylidene)pyridine-N-oxide-carbohydrazide).¹⁸ Colour code: Dy-aqua, O-red, N-blue, C-grey. Hydrogens are omitted for clarity. (b) Mechanism of relaxation of Dy1 center of **17** (Dy2 center is equivalent to Dy1 center). The red arrows indicate the QTM or TA-QTM via ground or excited KD, respectively. The sky dotted arrows shows the mechanism of Orbach process. The olive arrows indicate the pathway of magnetic relaxation.

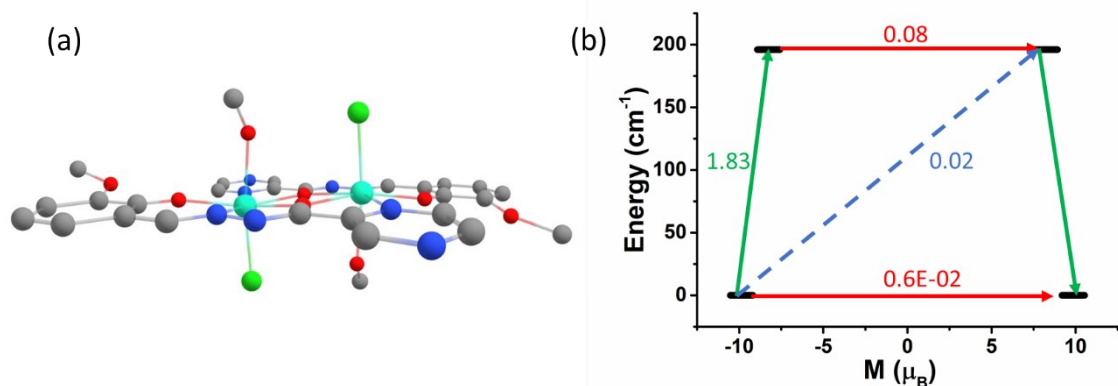


Figure S18: (a) Molecular structure of $[\text{Dy}(\text{opch})\text{Cl}(\text{MeOH})]_2$ (**18**).¹⁹ Colour code: Dy-aqua, Cl-green, O-red, N-blue, C-grey. Hydrogens are omitted for clarity. (b) Mechanism of relaxation of Dy1 center of **18** (Dy2 center is equivalent to Dy1 center). The Dy1 center relaxes via 1st excited KD due to the large angle (11.8°) of the anisotropy axis with respect to ground state despite of small TA-QTM at this level. The red arrows indicate the QTM or TA-QTM via ground or excited KD, respectively. The sky dotted arrows shows the mechanism of Orbach process. The olive arrows indicate the pathway of magnetic relaxation.

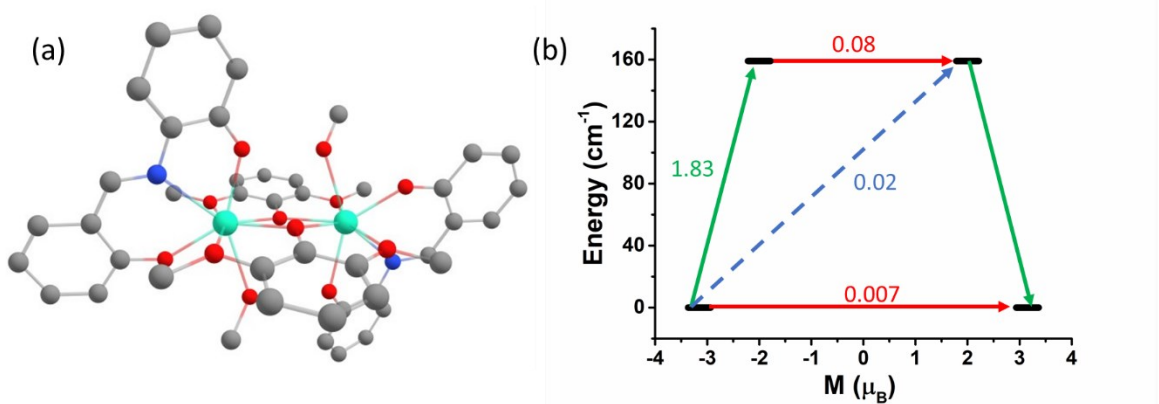


Figure S19: (a) Molecular structure of $[\text{Dy}_2(\text{L}_1)_2(\text{L}')_2(\text{CH}_3\text{OH})_2]$ (**19**, $\text{HL}' = 2,6\text{-dimethoxyphenol}$, $\text{H}_2\text{L}_1 = 2\text{-}((2\text{-hydroxybenzylidene})\text{amino})\text{phenol}$).²⁰ Colour code: Dy-aqua, O-red, N-blue, C-grey. Hydrogens are omitted for clarity. (b) Mechanism of relaxation of Dy1 center of **19** (Dy2 center is equivalent to Dy1 center). The Dy1 center relaxes via 1st excited KD due to the large angle (11.9°) of the anisotropy axis with respect to ground state despite of small TA-QTM at this level. The red arrows indicate the QTM or TA-QTM via ground or excited KD, respectively. The sky dotted arrows shows the mechanism of Orbach process. The olive arrows indicate the pathway of magnetic relaxation.

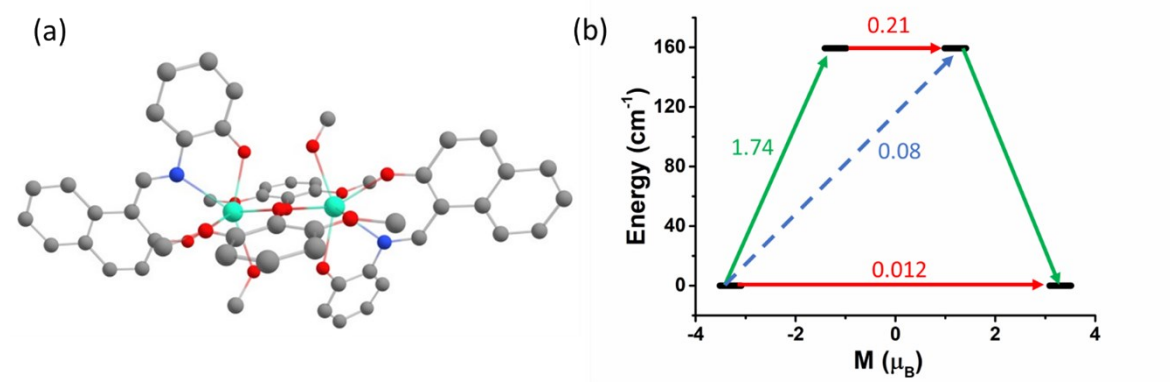


Figure S20: (a) Molecular structure of $[\text{Dy}_2(\text{L}_2)_2(\text{L}')_2(\text{CH}_3\text{OH})_2]$ (**20**, $\text{H}_2\text{L}_2 = 2-((2\text{-hydroxyphenyl})\text{imino})\text{-methyl)naphthalen-1-ol}$).²⁰ Colour code: Dy-aqua, O-red, N-blue, C-grey. Hydrogens are omitted for clarity. (b) Mechanism of relaxation of Dy1 center of **20** (Dy2 center is equivalent to Dy1 center). The red arrows indicate the QTM or TA-QTM via ground or excited KD, respectively. The sky dotted arrows shows the mechanism of Orbach process. The olive arrows indicate the pathway of magnetic relaxation.

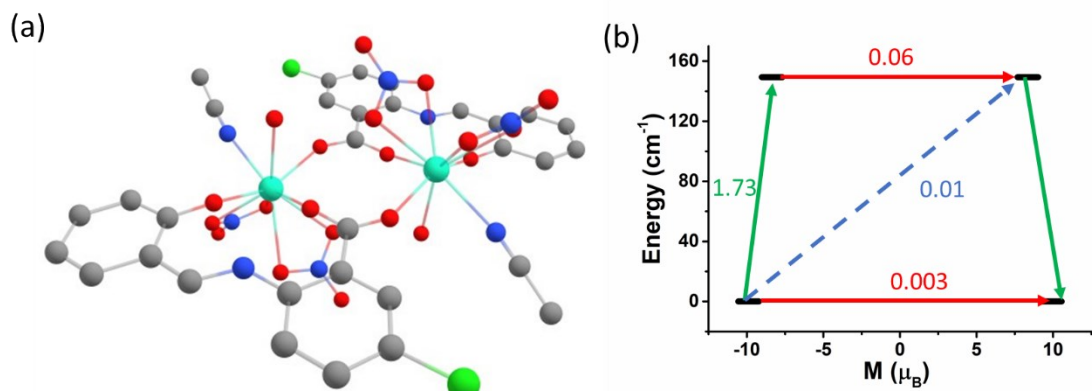


Figure S21: (a) Molecular structure of $[\text{Dy}_2(\text{NO}_3)_4(\text{sacbH}_2)_2(\text{H}_2\text{O})_2(\text{MeCN})_2]$ (**21**, $\text{sacbH}_2 = \text{N-salicylidene-2-amino-5-chlorobenzoic acid}$).²¹ Colour code: Dy-aqua, Cl-green, O-red, N-blue, C-grey. Hydrogens are omitted for clarity. (b) Mechanism of relaxation of Dy1 center of **21** (Dy2 center is equivalent to Dy1 center). The Dy1 center relaxes via 1st excited KD due to the large angle (9.2°) of the anisotropy axis with respect to ground state despite of small TA-QTM at this level. The red arrows indicate the QTM or TA-QTM via ground or excited KD, respectively. The sky dotted arrows shows the mechanism of Orbach process. The olive arrows indicate the pathway of magnetic relaxation.

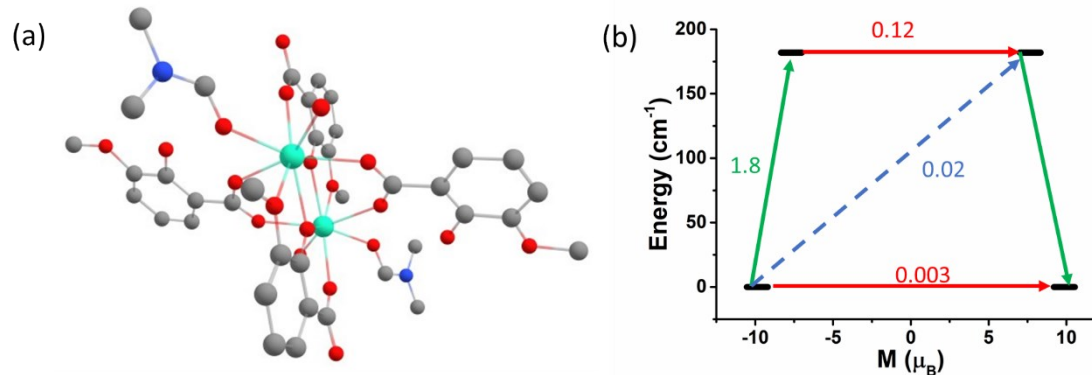


Figure S22: (a) Molecular structure of $[\text{Dy}_2\text{L}_2(\text{OAc})_4(\text{MeOH})_2]$ (**22**, $\text{HL} = (\text{E})\text{-N}'\text{-(2-hydroxybenzylidene)-2-mercaptopnicotinohydrazide}$).²² Colour code: Dy-aqua, Cl-green, O-red, N-blue, C-grey. Hydrogens are omitted for clarity. (b) Mechanism of relaxation of Dy1 center of **22** (Dy2 center is equivalent to Dy1 center). The red arrows indicate the QTM or TA-QTM via ground or excited KD, respectively. The sky dotted arrows shows the mechanism of Orbach process. The olive arrows indicate the pathway of magnetic relaxation.

(c) Dimer with organometallic building block:

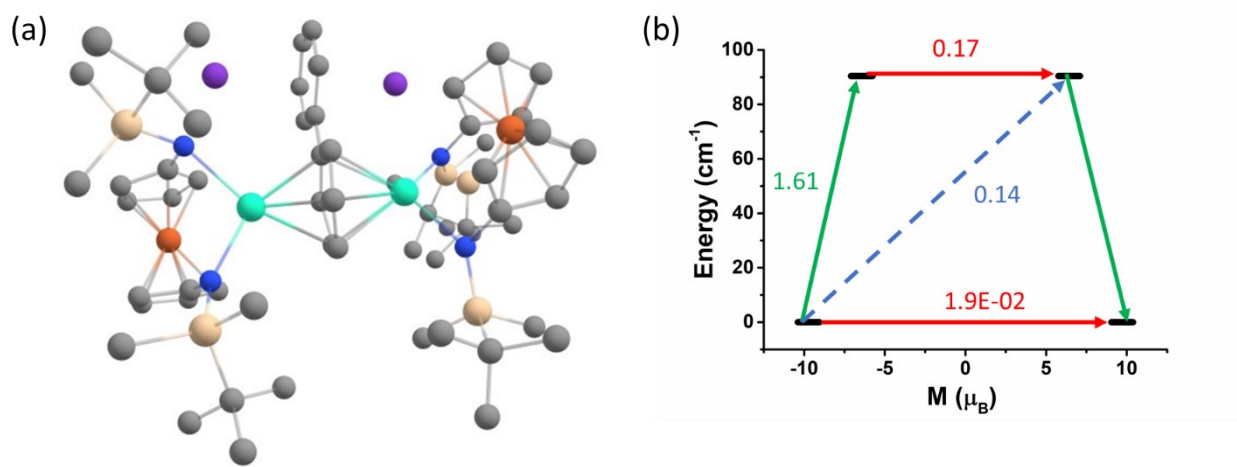


Figure S23: (a) Molecular structure of $[(\text{NN}^{\text{TBS}})\text{Dy}]_2(\mu\text{-biphenyl})[\text{K-(solvent)}]_2$ (**23**, $\text{NN}^{\text{TBS}} = 1,1\text{-(NSi}^{\text{t}}\text{BuMe}_2)_2$).²³ Colour code: Dy-aqua, Fe-redish brown, K-purple, Si-maple, O-red, N-blue, C-grey. Hydrogens are omitted for clarity. (b) Mechanism of relaxation of Dy1 center of **23** (Dy2 center is equivalent to Dy1 center). The red arrows indicate the QTM or TA-QTM via ground or excited KD, respectively. The sky dotted arrows shows the mechanism of Orbach process. The olive arrows indicate the pathway of magnetic relaxation.

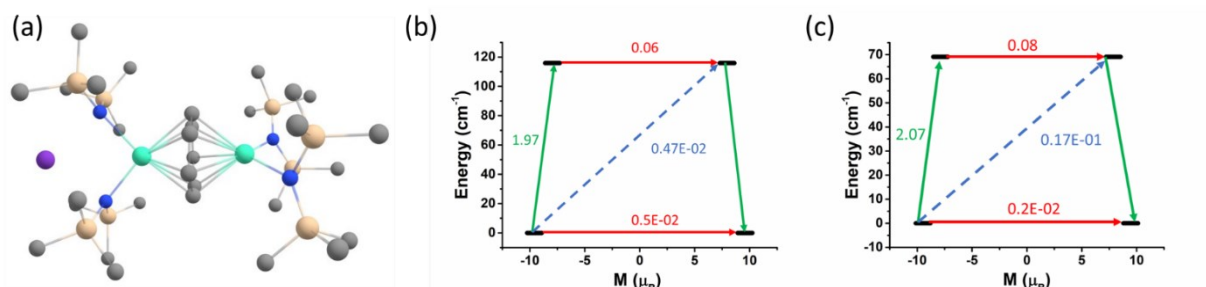


Figure S24: (a) Molecular structure of $[\text{KDy}_2(\text{C}_7\text{H}_7)(\text{N}(\text{SiMe}_3)_2)_4]$ (**24**).²⁴ Colour code: Dy-aqua, K-purple, Si-maple, O-red, N-blue, C-grey. Hydrogens are omitted for clarity. (b) Mechanism of relaxation of Dy1 center of

24. The Dy1 center relaxes via 1st excited KD due to the large angle (12.6°) of the anisotropy axis with respect to ground state despite of small TA-QTM at this level. (c) Mechanism of relaxation of Dy2 center of **24**. The Dy2 center relaxes via 1st excited KD due to the large angle (14.8°) of the anisotropy axis with respect to ground state despite of small TA-QTM at this level. The red arrows indicate the QTM or TA-QTM via ground or excited KD, respectively. The sky dotted arrows shows the mechanism of Orbach process. The olive arrows indicate the pathway of magnetic relaxation.

(d) **Dimers with μ -X⁻ (X = Cl, H) bridge:**

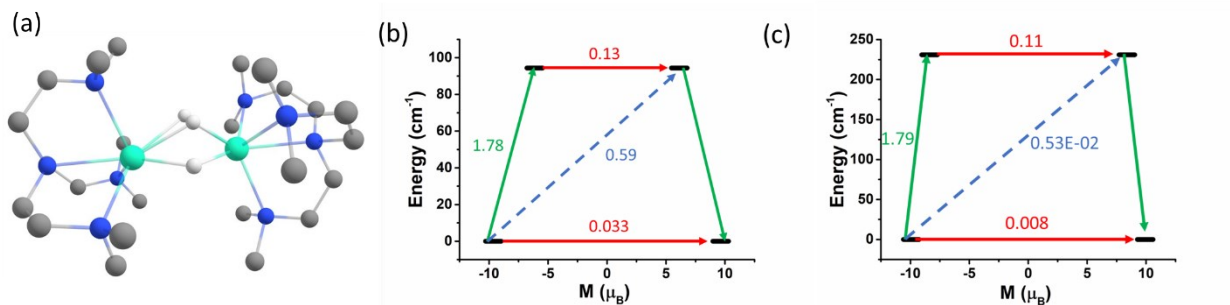


Figure S25: (a) Molecular structure of $[\text{Dy}(\text{Me}_6\text{trenCH}_2)(\mu\text{-H})_3\text{Dy}(\text{Me}_6\text{tren})]$ (**25**, $\text{Me}_6\text{tren} = \text{tris}\{2\text{-}(2\text{-dimethylamino)ethylamine}\}$).²⁵ Colour code: Dy-aqua, N-blue, C-grey, H-white. Hydrogens (except bridging hydrogens) are omitted for clarity. (b) Mechanism of relaxation of Dy1 center of **25**. The red arrows indicate the QTM or TA-QTM via ground or excited KD, respectively. The sky dotted arrows shows the mechanism of Orbach process. The olive arrows indicate the pathway of magnetic relaxation.

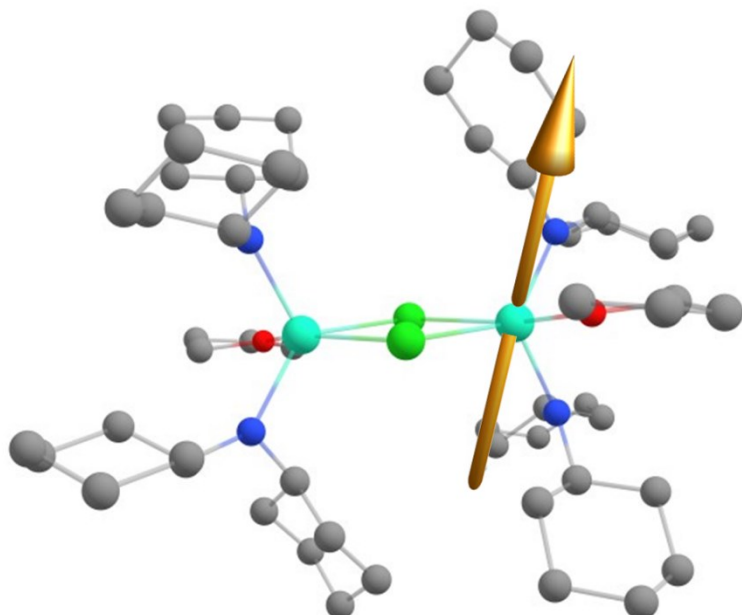


Figure S26: (a) The ground state anisotropy axis of Dy1 center of **26**.²⁶ Colour code: Dy-aqua, Cl-green, N-blue, C-grey. Hydrogens are omitted for clarity.

Table S5: The g tensors of eight KDs along with energy (cm^{-1}) of Dy1 center of **26** (Dy2 center is symmetric to Dy1).

Energy (cm^{-1})	g_x	g_y	g_z	Angle of g_{zz} between ground and higher excited KDs ($^{\circ}$)
0.0	0.000	0.000	19.863	
275.7	0.011	0.013	16.892	4.8
466.5	0.111	0.132	14.087	10.3
595.3	0.635	0.884	11.578	20.6
696.7	1.885	4.195	8.523	22.6
763.5	2.972	4.344	11.705	84.6
813.7	0.756	2.475	14.120	94.9
1024.4	0.010	0.017	19.495	91.9

(e) **Dimers with 2,2-bipyrimidine (bipym) bridge:**

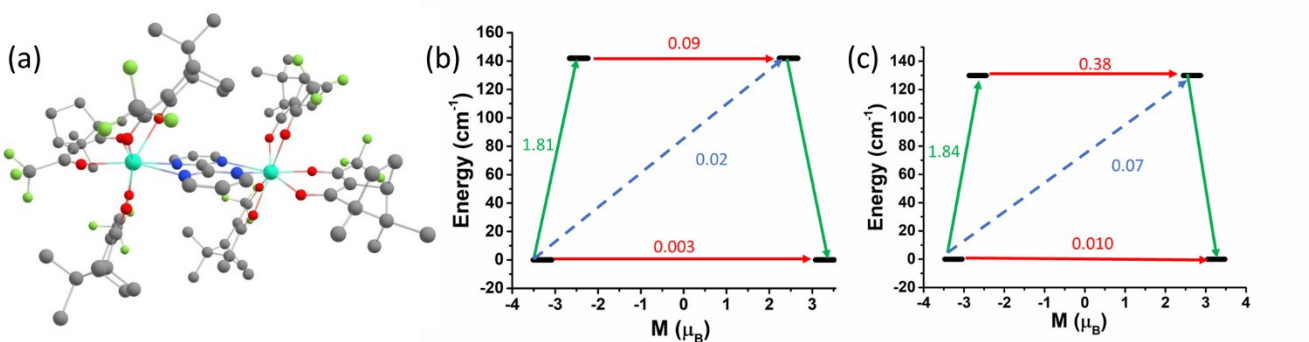
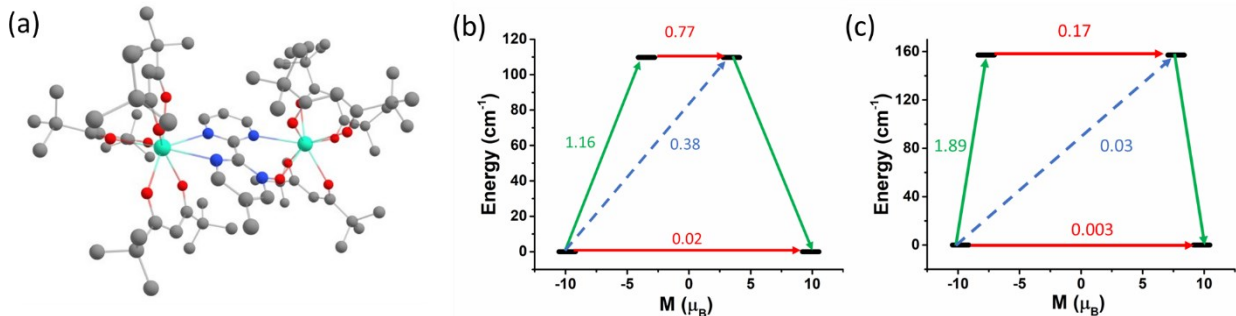


Figure S28: (a) Molecular structure of $[(\mu\text{-bipym})\{((+)\text{-tfacam})_3\text{Dy}\}_2]$ (**28**, tfacam = 3-(trifluoroacetyl)camphor).²⁸ Colour code: Dy-aqua, F-lime green, O-red, N-blue, C-grey, H-white. Hydrogens are omitted for clarity. (b) Mechanism of relaxation of Dy1 center of **28**. (c) Mechanism of relaxation of Dy2 center of **28**. The red arrows indicate the QTM or TA-QTM via ground or excited KD, respectively. The sky dotted arrows shows the mechanism of Orbach process. The olive arrows indicate the pathway of magnetic relaxation.

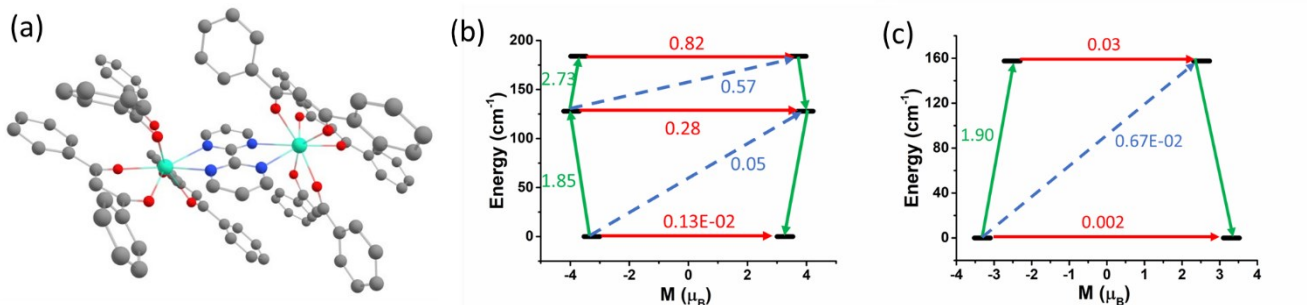


Figure S29: (a) Molecular structure of $[(\mu\text{-bipym})\{(\text{Dbzm})_3\text{Dy}\}_2]\cdot 2\text{CH}_3\text{Cl}$ (**29**, HDbzm = dibenzoylmethane).²⁹ Colour code: Dy-aqua, O-red, N-blue, C-grey, H-white. Hydrogens are omitted for clarity. (b) Mechanism of relaxation of Dy1 center of **29**. The Dy1 center does not relax via first excited KDs due to the large excitation coefficient from first excited to second excited KD which has been explained in the original paper. (c) Mechanism of relaxation of Dy2 center of **29**. The Dy2 center relaxes via 1st excited KD due to the large angle (14.8°) of the anisotropy axis with respect to ground state despite of small TA-QTM at this level. The red arrows indicate the QTM or TA-QTM via ground or excited KD, respectively. The sky dotted arrows shows the mechanism of Orbach process. The olive arrows indicate the pathway of magnetic relaxation.

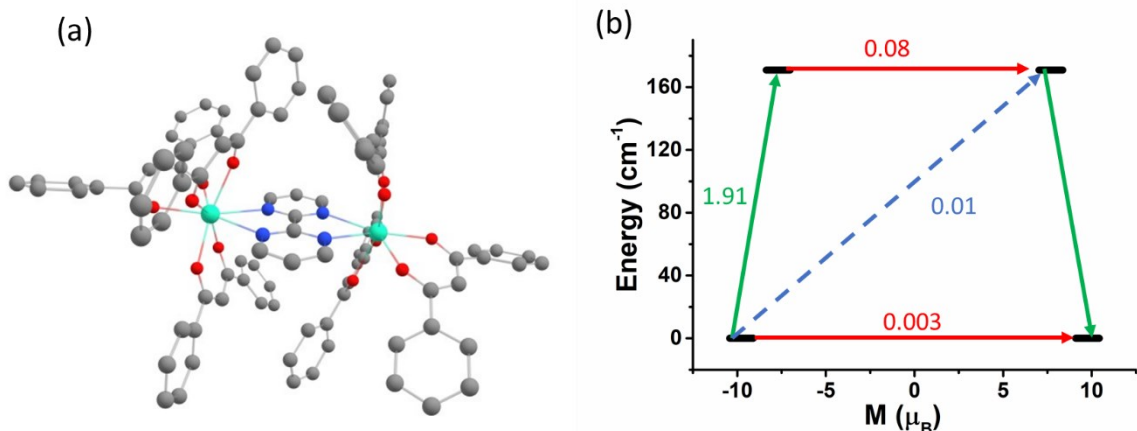


Figure S30: Molecular structure of $[(\mu\text{-bipym})\{(\text{Dbzm})_3\text{Dy}\}_2]\cdot\text{MeCN}$ (**30**).²⁹ Colour code: Dy-aqua, O-red, N-blue, C-grey, H-white. Hydrogens are omitted for clarity. (b) Mechanism of relaxation of Dy1 center of **30** (Dy2 center is equivalent to Dy1). The Dy1 center relaxes via 1st excited KD due to the large angle (6.1°) of the anisotropy axis with respect to ground state despite of small TA-QTM at this level. The red arrows indicate the QTM or TA-QTM via ground or excited KD, respectively. The sky dotted arrows shows the mechanism of Orbach process. The olive arrows indicate the pathway of magnetic relaxation.

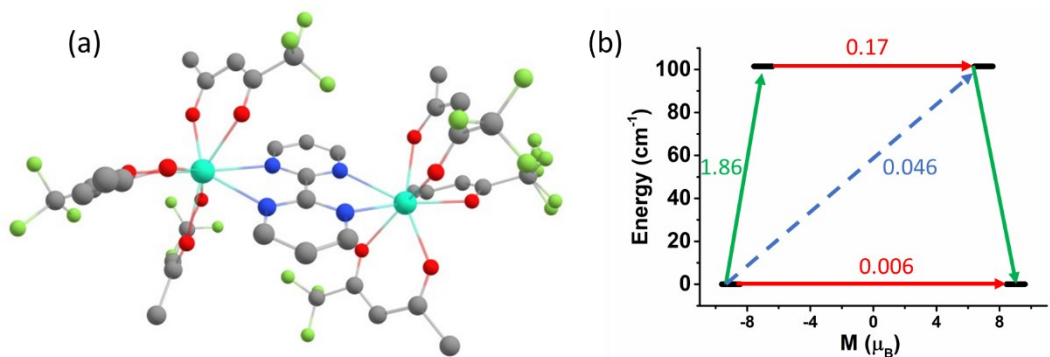


Figure S31: Molecular structure of $[\text{Dy}_2(\text{bpm})(\text{tfaa})_6]$ (31, tfaa = (1,1,1-trifluoroacetylacetone, bpm = 2,2'-bipyrimidine).³⁰ Colour code: Dy-aqua, F-lime green, O-red, N-blue, C-grey, H-white. Hydrogens are omitted for clarity. (b) Mechanism of relaxation of Dy1 center of 31 (Dy2 center is equivalent to Dy1). The red arrows indicate the QTM or TA-QTM via ground or excited KD, respectively. The sky dotted arrows shows the mechanism of Orbach process. The olive arrows indicate the pathway of magnetic relaxation.

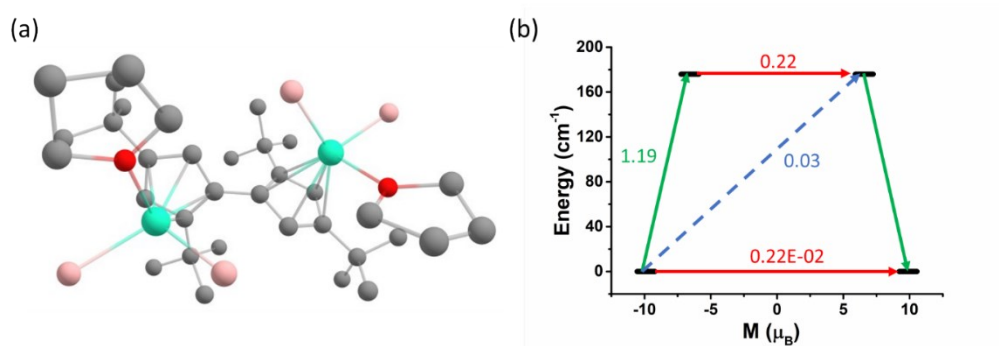


Figure S32: Molecular structure of 32.³¹ Colour code: Dy-aqua, B-light pink, O-red, C-grey. Hydrogens are omitted for clarity. (b) Mechanism of relaxation of Dy1 center of 32. The red arrows indicate the QTM or TA-QTM via ground or excited KD, respectively. The sky dotted arrows shows the mechanism of Orbach process. The olive arrows indicate the pathway of magnetic relaxation.

References:

1. L. Ungur and L. F. Chibotaru, *Inorg. Chem.*, 2016, **55**, 10043-10056.
2. F. Aquilante, J. Autschbach, R. K. Carlson, L. F. Chibotaru, M. G. Delcey, L. De Vico, I. Fdez. Galván, N. Ferré, L. M. Frutos and L. Gagliardi, *J. Comput. Chem.*, 2016, **37**, 506-541.
3. J. Liu, Y.-C. Chen, J.-L. Liu, V. Vieru, L. Ungur, J.-H. Jia, L. F. Chibotaru, Y. Lan, W. Wernsdorfer and S. Gao, *J. Am. Chem. Soc.*, 2016, **138**, 5441-5450.
4. Y.-N. Guo, G.-F. Xu, W. Wernsdorfer, L. Ungur, Y. Guo, J. Tang, H.-J. Zhang, L. F. Chibotaru and A. K. Powell, *J. Am. Chem. Soc.*, 2011, **133**, 11948-11951.

5. R. J. Blagg, L. Ungur, F. Tuna, J. Speak, P. Comar, D. Collison, W. Wernsdorfer, E. J. McInnes, L. F. Chibotaru and R. E. Winpenny, *Nat. Chem.*, 2013, **5**, 673-678.
6. K. R. Vignesh, D. I. Alexandropoulos, B. S. Dolinar and K. R. Dunbar, *Dalton Trans.*, 2019, **48**, 2872-2876.
7. M. Lines, *The Journal of Chemical Physics*, 1971, **55**, 2977-2984.
8. L. F. Chibotaru, L. Ungur and A. Soncini, *Angew. Chem.*, 2008, **120**, 4194-4197.
9. S. A. Sulway, R. A. Layfield, F. Tuna, W. Wernsdorfer and R. E. Winpenny, *ChemComm*, 2012, **48**, 1508-1510.
10. F. Tuna, C. A. Smith, M. Bodensteiner, L. Ungur, L. F. Chibotaru, E. J. McInnes, R. E. Winpenny, D. Collison and R. A. Layfield, *Angew. Chem. Int. Ed.*, 2012, **51**, 6976-6980.
11. C. P. Burns, B. O. Wilkins, C. M. Dickie, T. P. Latendresse, L. Vernier, K. R. Vignesh, N. S. Bhuvanesh and M. Nippe, *ChemComm*, 2017, **53**, 8419-8422.
12. Y.-S. Meng, J. Xiong, M.-W. Yang, Y.-S. Qiao, Z.-Q. Zhong, H.-L. Sun, J.-B. Han, T. Liu, B.-W. Wang and S. Gao, *Angew. Chem. Int. Ed.*, 2020, **59**, 13037-13043.
13. D. Errulat, B. Gabidullin, A. Mansikkamaki and M. Murugesu, *ChemComm*, 2020, **56**, 5937-5940.
14. P. Evans, D. Reta, C. A. P. Goodwin, F. Ortú, N. F. Chilton and D. P. Mills, *ChemComm*, 2020, **56**, 5677-5680.
15. J. Long, F. Habib, P.-H. Lin, I. Korobkov, G. Enright, L. Ungur, W. Wernsdorfer, L. F. Chibotaru and M. Murugesu, *J. Am. Chem. Soc.*, 2011, **133**, 5319-5328.
16. F. Habib, G. Brunet, V. Vieru, I. Korobkov, L. F. Chibotaru and M. Murugesu, *J. Am. Chem. Soc.*, 2013, **135**, 13242-13245.
17. H. Tian, L. Ungur, L. Zhao, S. Ding, J. Tang and L. F. Chibotaru, *Chem. Eur. J.*, 2018, **24**, 9928-9939.
18. F. Ma, Q. Chen, J. Xiong, H.-L. Sun, Y.-Q. Zhang and S. Gao, *Inorg. Chem.*, 2017, **56**, 13430-13436.
19. H. Tian, B.-L. Wang, J. Lu, H.-T. Liu, J. Su, D. Li and J. Dou, *ChemComm*, 2018, **54**, 12105-12108.
20. S. Mukherjee, J. Lu, G. Velmurugan, S. Singh, G. Rajaraman, J. Tang and S. K. Ghosh, *Inorg. Chem.*, 2016, **55**, 11283-11298.
21. E. C. Mazarakioti, J. Regier, L. Cunha-Silva, W. Wernsdorfer, M. Pilkington, J. Tang and T. C. Stamatatos, *Inorg. Chem.*, 2017, **56**, 3568-3578.
22. L. Zhong, W.-B. Chen, X.-H. Li, Z.-J. OuYang, M. Yang, Y.-Q. Zhang, S. Gao and W. Dong, *Inorg. Chem.*, 2020, **59**, 4414-4423.
23. W. Huang, J. J. Le Roy, S. I. Khan, L. Ungur, M. Murugesu and P. L. Diaconescu, *Inorg. Chem.*, 2015, **54**, 2374-2382.
24. K. L. Harriman, J. J. Le Roy, L. Ungur, R. J. Holmberg, I. Korobkov and M. Murugesu, *Chem. Sci.*, 2017, **8**, 231-240.
25. A. Venugopal, F. Tuna, T. P. Spaniol, L. Ungur, L. F. Chibotaru, J. Okuda and R. A. Layfield, *ChemComm*, 2013, **49**, 901-903.
26. T. Han, Y.-S. Ding, Z.-H. Li, K.-X. Yu, Y.-Q. Zhai, N. F. Chilton and Y.-Z. Zheng, *ChemComm*, 2019, **55**, 7930-7933.
27. I. F. Díaz-Ortega, J. M. Herrera, D. Aravena, E. Ruiz, T. Gupta, G. Rajaraman, H. Nojiri and E. Colacio, *Inorg. Chem.*, 2018, **57**, 6362-6375.
28. I. F. Díaz-Ortega, J. M. Herrera, Á. Reyes Carmona, J. R. Galán-Mascarós, S. Dey, H. Nojiri, G. Rajaraman and E. Colacio, *Front. Chem.*, 2018, **6**, 537.
29. W.-B. Sun, B. Yan, L.-H. Jia, B.-W. Wang, Q. Yang, X. Cheng, H.-F. Li, P. Chen, Z.-M. Wang and S. Gao, *Dalton Trans.*, 2016, **45**, 8790-8794.
30. D. Errulat, R. Marin, D. A. Gállico, K. L. Harriman, A. Pialat, B. Gabidullin, F. Iikawa, O. D. Couto Jr, J. O. Moilanen and E. Hemmer, *ACS Cent. Sci.*, 2019, **5**, 1187-1198.
31. M. He, F. S. Guo, J. Tang, A. Mansikkamaki and R. A. Layfield, *Chem Sci*, 2020, **11**, 5745-5752.

